Journal of Dynamical Systems and Complexity (2026) vol.1(2): 15-27
eISSN: 3122-4326, DOI: 10.66131/JDSC12202615-27

On The Synchronization Of Dynamical Systems With Hidden Attractors

Juan Gonzalo Barajas-Ramírez[1]*

[1]IPICYT, División de Control y Sistemas Dinámicos
Camino a la Presa San José 2055, Lomas 4ta,
CP 78216, San Luis Potosí, S. L. P., México.

Abstract

We use Lyapunov-based analysis to investigate the emergence of synchronization in systems with self-excited and hidden attractors. When these types of attractors coexist, synchronizing systems on a hidden attractor is a challenging open problem. Our results show that, for systems with coexisting attractors in a drive-response configuration, it is relatively simple to impose a synchronized behavior on a hidden attractor; however, in the bidirectional configuration, the hidden attractors basically disappear, with the synchronized solution converging towards a self-excited attractor for any coupling strength. We illustrate our results with numerical simulations of many well-known systems with hidden and self-excited attractors.

Keywords— Synchronization, Hidden Attractors, Stability Analysis

1 Introduction

Nonlinear systems may exhibit a variety of complex behaviors. As their trajectories move through state space, they approach and recede from invariant sets; the geometric objects to which they contract are called attractors. Furthermore, the region of state space from which flows converge to a given attractor is called its basin of attraction [1]. A self-excited attractor emerges on the intersection between the manifolds of an unstable equilibrium point and its basin of attraction. In recent years, an alternative class of attractors has been identified; namely, hidden attractors, which are attractors whose basins of attraction do not intersect the manifolds of unstable equilibrium points [2].

From the general description above, hidden attractors can be found in systems without equilibrium points, with an infinite number of equilibria, or with at least one stable equilibrium. Moreover, as shown in [3], hidden and self-excited attractors can coexist in the same dynamical system.

Hidden attractors are inherently complex to identify because trajectories starting near an equilibrium point will not move towards the hidden attractor. However, the literature contains numerous examples of dynamical systems with hidden attractors. One of the earlier examples comes from the set of simple chaotic flows proposed by Sprott in the 90s [4]. From case A in this reference, a plethora of systems without equilibrium points with hidden attractors were proposed in [5, 6]. Other authors have investigated the existence of hidden attractors in dynamical systems with an infinite number of equilibrium points [7, 8]. Other examples of dynamical systems with hidden attractors that have stable equilibrium points are found in [9, 10]. Furthermore, for many systems, both types of attractors coexist [2, 3, 11, 12].

Most of the examples above have nonlinearities with quadratic and higher-order terms. However, simpler versions of systems with hidden attractors are derived from piecewise linear (PWL) systems [2, 13, 14]. An analytical-numerical methodology can be used to identify hidden attractors in nonlinear dynamical systems. Using harmonic linearization and describing functions, the existence of hidden oscillatory solutions can be found [11]. Using these ideas, self-excited and hidden attractors can be identified for the same dynamical system [3].

Synchronization is a universal and widely studied nonlinear phenomenon. In general terms, two or more dynamical systems that interact through a subtle coupling are said to be synchronized when their behaviors are correlated in time [15]. Depending on the features of their temporal correlation, many different types of synchronized behaviors can be defined, including: identical, phase, anti-phase, and generalized synchronization, to mention but a few [16].

A critical component of synchronization is the interaction between systems. Perhaps the simplest form of interaction is the so-called drive-response configuration [17]. In this case, the one-directional interconnection can

*Corresponding author: jgbarajas@ipicyt.edu.mx
Received: January 15, 2026, **Published:** June 1, 2026
Edited by E. Campos-Cantón

easily be interpreted, from the viewpoint of control theory, as a feedback control problem where the coupling term in the response subsystem can be designed using different methodologies like robust [18], adaptive [19], and optimal control techniques to achieve synchronization [20]. Alternatively to a drive-response configuration, two dynamical systems can be bidirectionally coupled. In general terms, in this configuration, the synchronization problem is more complex since both subsystems depend on each other through their interactions [16]. Solutions to the bidirectional synchronization problem have naturally been extended to the context of dynamical networks [21], where problems such as consensus and pinning are significant research topics [22].

In this contribution, we investigate the synchronization problem of dynamical systems with self-excited and hidden attractors. In particular, as observed in [3, 23], when coexisting hidden and self-excited attractors are present, the emergence of synchronized behavior on the hidden attractor is not readily achieved. We find that synchronization of the hidden attractor is possible in the drive-response configuration; however, bidirectional synchronization is almost impossible to achieve. We attribute the observed difficulty in achieving synchronization to the differences in the sizes of their basins of attraction and to the proximity of their attractors in state space. On the other hand, in the case of a hidden attractor due to non-equilibrium systems, synchronization is achieved regardless of the size of their basin of attraction.

The remainder of this contribution is organized as follows. In Section 2, we provide some examples of dynamical systems with hidden attractors of different natures. In Section 3, we describe the synchronization problem for drive-response and bidirectional configurations, along with an output-feedback design solution. In Section 4, we use numerical simulations to illustrate our main results. Then, we provide some closing remarks.

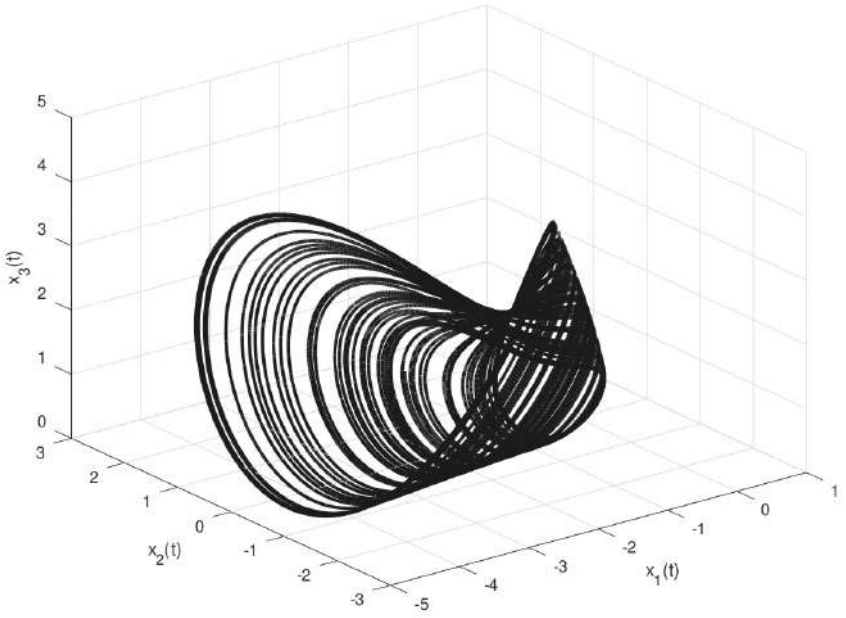

Figure 1: Hidden attractor of the system without equilibrium points (1) from the initial condition $[-1.6, 0.82, 1.9]^\top$

2 Hidden attractors of dynamical systems

By definition, any attractor of a dynamical system without equilibrium points is hidden. For example, the following modification of the Sprott system case A [5]:

$$\begin{aligned} \dot{x}_1(t) &= -x_2(t), \\ \dot{x}_2(t) &= x_1(t) + x_3(t), \\ \dot{x}_3(t) &= 2x_2(t)^2 + x_1(t)x_3(t) - 0.35 \end{aligned} \tag{1}$$

results in the hidden attractor shown in Figure 1.

An example of dynamical systems with hidden attractors and stable equilibrium points is [9]:

$$\begin{aligned} \dot{x}_1(t) &= x_2(t)x_3(t) + 0.006, \\ \dot{x}_2(t) &= x_1(t)^2 - x_2(t), \\ \dot{x}_3(t) &= 1 - 4x_1(t), \end{aligned} \tag{2}$$

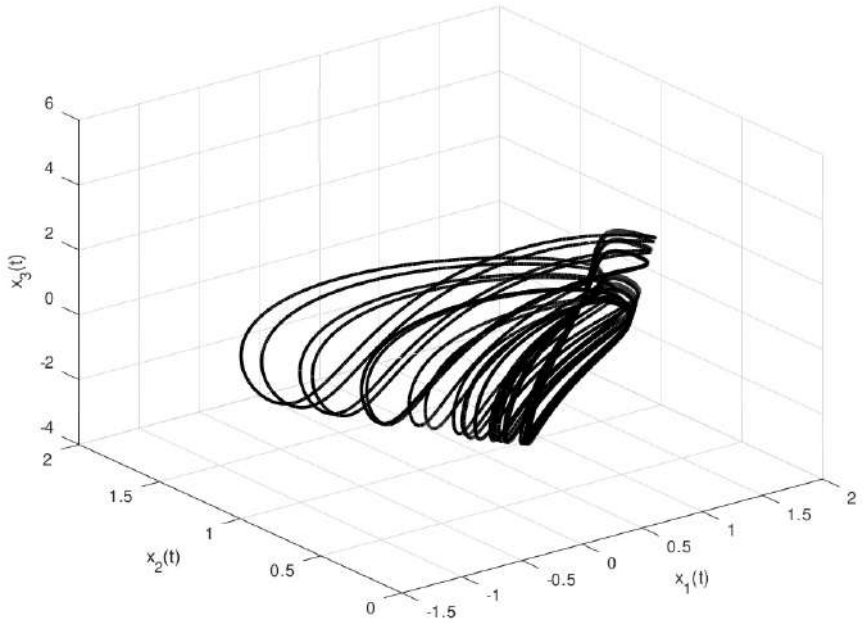

Figure 2: Hidden attractor of the system with a stable equilibrium point (2) from the initial condition $[0.1, 0.1, 0.1]^\top$

which has the asymptotically stable equilibrium point $x_{eq} = [0.25, 0.0625, -0.096]^\top$ and as shown in Figure 2 a hidden attractor.

Other variants of systems with hidden attractors have lines of equilibrium points like [8]:

$$\begin{aligned} \dot{x}_1(t) &= x_2(t), \\ \dot{x}_2(t) &= -x_1(t) + x_2(t)x_3(t), \\ \dot{x}_3(t) &= -x_1(t) - 15x_1(t)x_2(t) - x_1(t)x_3(t) \end{aligned} \tag{3}$$

which has a line of stable equilibrium points at $[0, 0, x_3^*]^\top$ with $x_3^* \in \mathbf{R}$ and the hidden attractor shown in Figure 3.

The three previous variants of hidden attractor are possible using the appropriate values of the parameters a, b, and c for the system [24]:

$$\begin{aligned} \dot{x}_1(t) &= x_2(t), \\ \dot{x}_2(t) &= 0.4x_1(t)x_3(t) - a, \\ \dot{x}_3(t) &= 0.3x_2(t) - 0.1x_3(t) - 1.4x_2^2(t) - bx_1(t)x_2(t) - c, \end{aligned} \tag{4}$$

In the study of hidden attractors, Chua's circuit is a critical tool. Recent investigations have revealed that in addition to its self-excited chaotic attractor, there are coexisting hidden attractors in the system [2, 3]:

$$\begin{aligned} \dot{x}_1(t) &= \alpha(x_2(t) - x_1(t)(m_1 + 1) - \psi(x_1(t))), \\ \dot{x}_2(t) &= x_1(t) - x_2(t) + x_3(t), \\ \dot{x}_3(t) &= -(\beta x_2(t) + \gamma x_3(t)). \end{aligned} \tag{5}$$

where $\psi(x_1(t)) = \frac{1}{2}(m_0 - m_1)(|x_1(t) + 1| - |x_1(t) - 1|)$. For the parameter values $\alpha = 9.3516$, $\beta = 14.7903$, $\gamma = 0.0161$, $m_0 = -0.7225$ and $m_1 = -1.1384$ the system (5) results in the self-excited chaotic attractor shown in Figure 4. While for the values $\alpha = 8.4562$, $\beta = 12.0732$, $\gamma = 0.0052$, $m_0 = -0.1768$ and $m_1 = -1.1468$ the system (5) has the two coexisting hidden attractors shown in Figure 5.

An interpretation of Chua's circuit is as a continuously connected PWL system. Using this interpretation as inspiration, many different hidden attractors have been found in PWL systems [12]. On the other hand, the Sprott systems can be interpreted as generated from the Jerk equation with a nonlinear component [4, 25]. Therefore, combining these ideas, one can find hidden attractors in systems based on the Jerk equation with PWL nonlinearities, like the following system:

$$\begin{bmatrix} \dot{x}_1(t) \\ \dot{x}_2(t) \\ \dot{x}_3(t) \end{bmatrix} = \begin{bmatrix} 0 & 1 & 0 \\ 0 & 0 & 1 \\ -0.7 & -0.5 & -1 \end{bmatrix} \begin{bmatrix} x_1(t) \\ x_2(t) \\ x_3(t) \end{bmatrix} + \begin{bmatrix} 0 \\ 0 \\ 1 \end{bmatrix} F(x_1(t)) \tag{6}$$

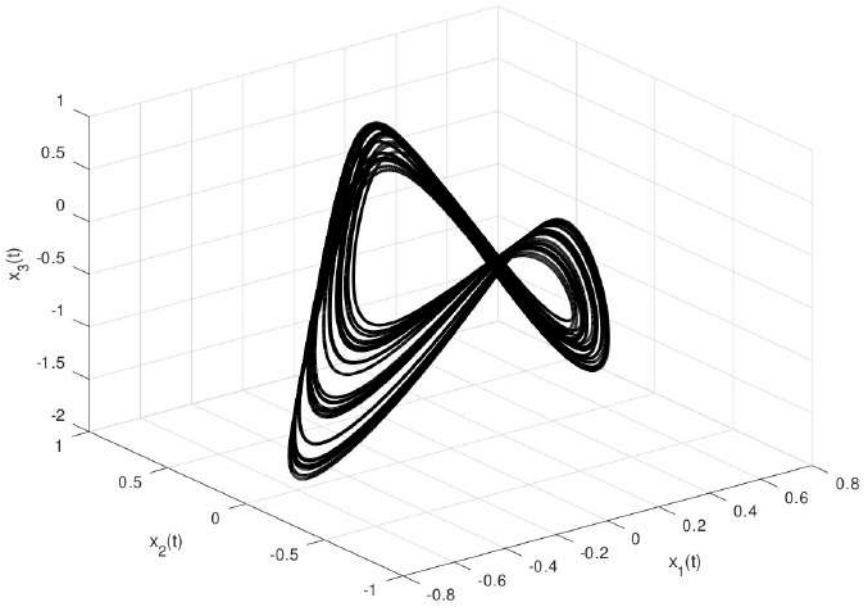

Figure 3: Hidden attractor of the system with a line of stable equilibrium points (3) from the initial condition $[0, 0.5, 0.5]^\top$

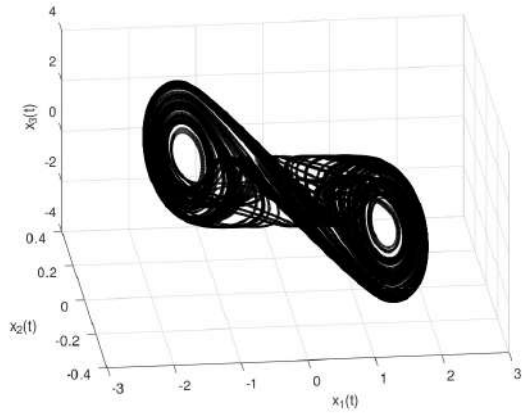

Figure 4: Self-excited chaotic attractor for Chua's circuit (5) from the initial condition $[0.1, 0.1, 0.1]^\top$

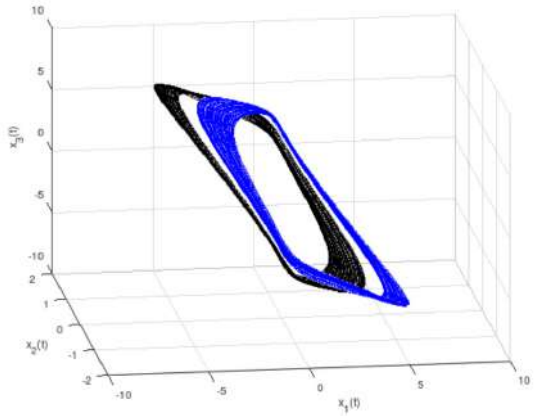

Figure 5: Coexisting hidden attractors for Chua's circuit (5) from the initial conditions $[\pm 3.7725, \pm 1.3511, \mp 4.6657]^\top$

with $F(x_1(t)) = \frac{1}{2}(1.5 - 5.0)(|x_1(t) + 1| - |x_1(t) - 1|$, which results in the self-excited attractor shown in Figure 6 and the coexisting hidden attractors in Figure 7.

In the following Section, we describe a solution to the synchronization problem in both the drive-response and bidirectional configurations.

3 The synchronization problem

Consider two coupled identical dynamical systems:

$$\begin{aligned} \dot{x}(t) &= F(x(t)) + K_1(w(t), z(t)) \\ w(t) &= Cx(t) \end{aligned} \tag{7}$$

$$\begin{aligned} \dot{y}(t) &= F(y(t)) + K_2(w(t), z(t)) \\ z(t) &= Cy(t) \end{aligned} \tag{8}$$

where $x(t), y(t) \in \mathbf{R}^3$ are the state variables; $F(\cdot) : \mathbf{R}^3 \to \mathbf{R}^3$ describes the system's dynamics, which are nonlinear and at least locally Lipschitz. The variables $w(t) \in \mathbf{R}$ and $z(t) \in \mathbf{R}$ are the outputs of the corresponding systems

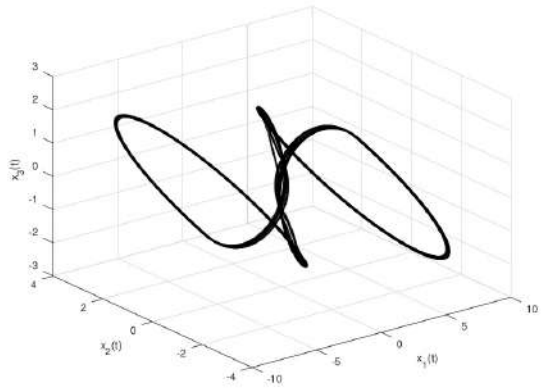

Figure 6: Self-excited attractor for the Jerk equation based system (6) from the initial condition $[0.1, 0.1, 0.1]^\top$

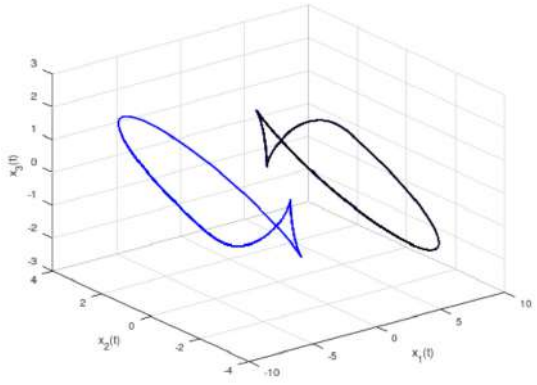

Figure 7: Coexisting hidden attractors for (6) from the initial conditions $[\mp 0.9488, \pm 2.1717, \mp 2.1652]^\top$

with $C \in \mathbf{R}^{1\times 3}$. While the coupling functions $K_i(\cdot,\cdot) : \mathbf{R}^6 \to \mathbf{R}^3$ for $i = 1, 2$ are to be design such that:

$$\lim_{t\to\infty} ||x(t) - y(t)|| = 0 \tag{9}$$

In other words, the coupling functions $K_i(\cdot,\cdot)$ are to be design such that systems (7) and (8) *asymptotically* achieve *identical synchronization*. As shown in Figure 8 and 9, we have two coupling configurations:

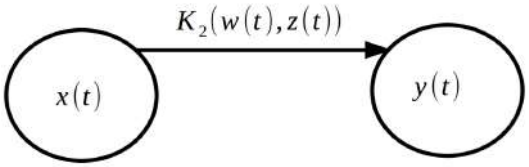

Figure 8: Drive-response scheme

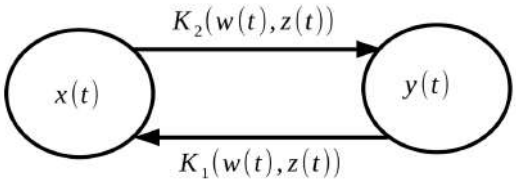

Figure 9: Bidirectional scheme

- **Drive-Response** configuration (Figure 8) which correspond to the coupled system (7)-(8) with $K_1(\cdot,\cdot) = 0$ and $K_2(\cdot,\cdot) \neq 0$
- **Bidirectional** coupling configuration (Figure 9) for the coupled systems (7) and (8) with $K_1(\cdot,\cdot) \neq 0$ and $K_2(\cdot,\cdot) \neq 0$

Additionally, these coupling functions are assumed to be linear combinations of the difference between the system's outputs, *i.e.*, diffusive symmetric output coupling:

$$\begin{aligned} K_1(w(t),z(t)) &= \kappa_1(w(t) - z(t)) = \kappa_1 C(y(t) - x(t)) \\ K_2(w(t),z(t)) &= \kappa_2(z(t) - w(t)) = \kappa_2 C(x(t) - y(t)) \end{aligned} \tag{10}$$

where $\kappa_i \in \mathbf{R}^{3\times 1}$ for $i = 1, 2$ are the coupling gains that are to be designed such that (9) is satisfied.

3.1 Synchronization on a drive-response scheme

To verify the emergence of identical synchronization in (7)-(8), in the sense of (9), we define the error variables:

$$\begin{aligned} e_1(t) &= x(t) - y(t) \\ e_2(t) &= y(t) - x(t). \end{aligned} \tag{11}$$

with $e_1(t) = -e_2(t)$.

In the drive-response configuration, since $K_1(\cdot,\cdot) = 0$, we have the error dynamics:

$$\dot{e}_1(t) \quad = \quad F_1 - \kappa_2 C(y(t) - x(t)) = F_1 - \kappa_2 C e_1(t) \tag{12}$$

where $F_1 = F(x(t)) - F(y(t))$. Then, if the error dynamics (12) are at least locally asymptotically stable the *drive-response* coupled systems (7)-(8) will synchronize.

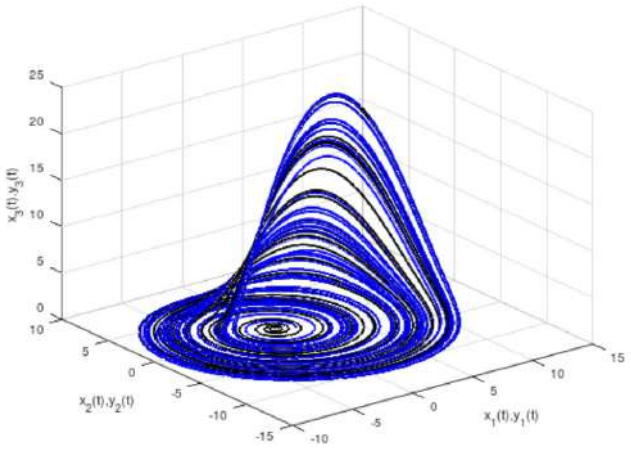

(a) Self-excited chaotic attractor of the Rössler system (29)

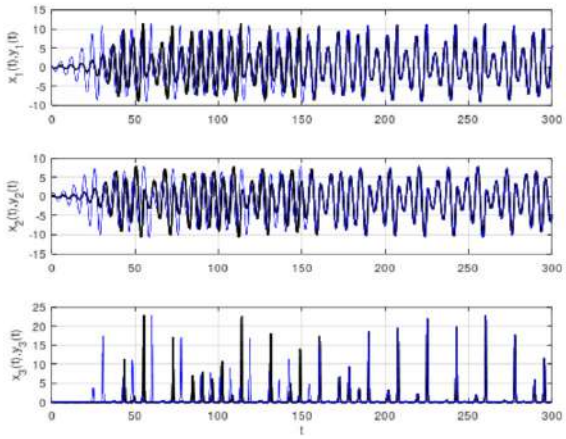

(b) State variables of the drive-response coupled Rössler systems

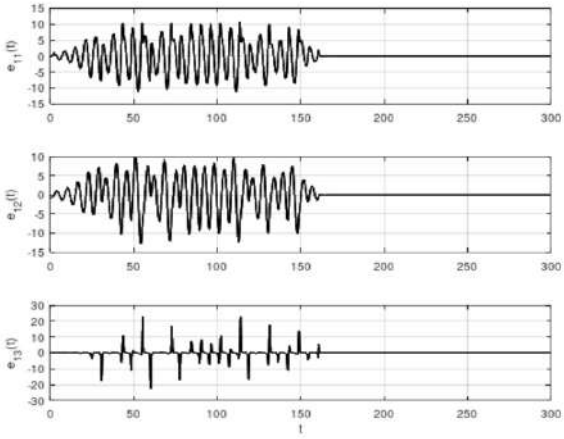

(c) Synchronization error for the drive-response coupled Rössler systems

Figure 10: Synchronization of coupled Rössler systems in drive-response configuration with $\kappa_2 = 0.5$ for $t > 150$

The stability of (12) can establish using the Lyapunov function

$$V(e_1(t)) = e_1(t)^\top P e_1(t) \tag{13}$$

with $P = P^\top > 0$ a positive definitive matrix. Its derivative along the trajectories of (12) is:

$$\dot{V}(e_1(t)) = F_1^\top P e_1(t) + e_1(t)^\top P F_1 - e_1(t)^\top [(\kappa_2 C)^\top P + P\kappa_2 C] e_1(t)) \tag{14}$$

Under the assumption that:

$$P(F(x(t)) - F(y(t))) \leq LP(x(t) - y(t)) \tag{15}$$

with $L \in \mathbf{R}$. The derivative of this Lyapunov function is bounded by

$$\dot{V}(e_1(t)) \leq e_1(t)^\top Q e_1(t) \tag{16}$$

with $Q = 2LP - (\kappa_2 C)^\top P + P\kappa_2 C$. For the error dynamics (12) to be locally asymptotically stable we need to have Q as a negative definitive matrix, that is:

$$2LP - (\kappa_2 C)^\top P + P\kappa_2 C < -\tau I_3 \tag{17}$$

with $\tau > 0$ and I_3 the square identity matrix of dimension three. Then, by choosing κ_2 such that (17) is satisfied the drive-response coupled system (7)-(8) will synchronize.

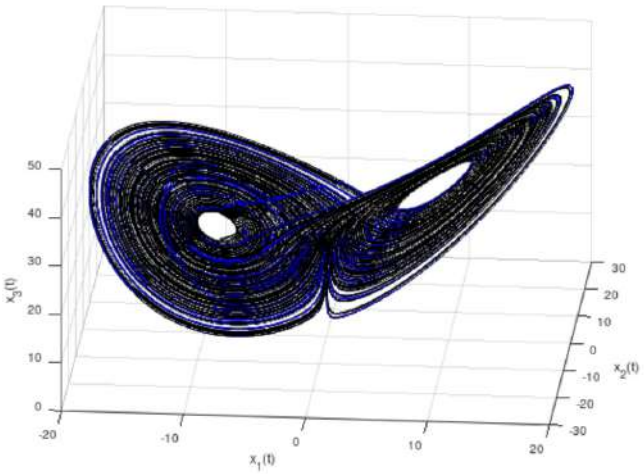

(a) Self-excited chaotic attractor of the Lorenz system (31)

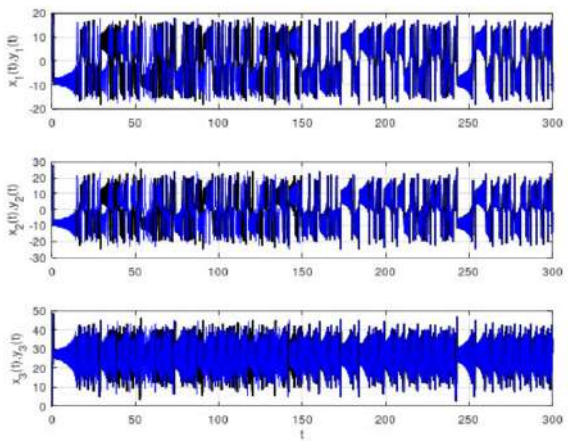

(b) State variables of the bidirectionally coupled Lorenz systems

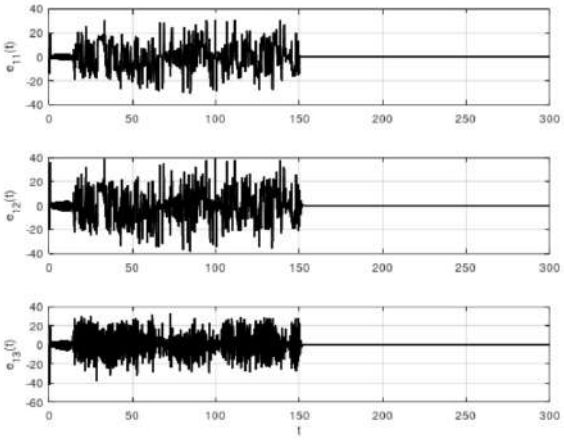

(c) Deviation error for the bidirectionally coupled Lorenz systems with $\kappa_{11} = 50$ for $t > 150$

Figure 11: Synchronization of coupled Lorenz systems in bidirectional configuration with $\kappa_{11} = 50$ for $t > 150$

3.2 Synchronization on a bidirectionally coupled scheme

In the bidirectionally coupled configuration, the error dynamics are:

$$\begin{array}{rcl} \dot{e}_1(t) & = & F_1 + \kappa_1 C e_2(t) - \kappa_2 C e_1(t) \\ \dot{e}_2(t) & = & F_2 + \kappa_2 C e_1(t) - \kappa_1 C e_2(t) \end{array} \tag{18}$$

with $F_2 = F(y(t)) - F(x(t))$. For simplicity, let $\kappa_1 = \kappa_2 = \kappa \in \mathbf{R}^3$, then when synchronization is achieved, we have a solution for the coupled systems where:

$$x(t) = y(t) = s(t) \tag{19}$$

That is, when the systems are synchronized, the coupling functions in (10) are zero, and each node moves as:

$$\dot{s}(t) \quad = \quad F(s(t)) \tag{20}$$

We define a set of error variables to describe its deviation from the synchronized solution as:

$$\begin{array}{l} \epsilon_1(t) = x(t) - s(t) \\ \epsilon_2(t) = y(t) - s(t). \end{array} \tag{21}$$

Then, the deviation error dynamics are:

$$\begin{array}{rcl} \dot{\epsilon}_1(t) & = & F_{1s} + \kappa C \epsilon_2(t) - \kappa C \epsilon_1(t) \\ \dot{\epsilon}_2(t) & = & F_{2s} + \kappa C \epsilon_1(t) - \kappa C \epsilon_2(t) \end{array} \tag{22}$$

where $F_{1s} = F(x(t)) - F(s(t))$ and $F_{2s} = F(y(t)) - F(s(t))$. That in vector form becomes:

$$\dot{E}(t) \quad = \quad \mathbf{F} + (A \otimes \kappa C)E(t) \tag{23}$$

where $E(t) = \begin{bmatrix} \epsilon_1(t) \\ \epsilon_2(t) \end{bmatrix} \in \mathbf{R}^6$, $\mathbf{F} = \begin{bmatrix} F_{1s} \\ F_{2s} \end{bmatrix} : \mathbf{R}^6 \to \mathbf{R}^6$, $A = \begin{bmatrix} -1 & 1 \\ 1 & -1 \end{bmatrix}$ is the Laplacian matrix of the *bidirectional* connection, and $\otimes$ represents the Kronecker product.

Synchronization of the bidirectionally coupled systems (7)-(8) is achieved if the deviation error dynamics (23) are at least locally asymptotically stable around their zero solution.

Stability of the deviation error is investigated linearizing (23) at the zero solution, which results in:

$$\dot{E}(t) \quad = \quad [D\mathbf{F}(s(t)) + (A \otimes \kappa C)]\, E(t) \tag{24}$$

where $D\mathbf{F}(s(t)) = [DF(s(t)), DF(s(t))]^\top$ with $DF(\cdot)$ the Jacobian matrix of the system's dynamics. Since A is a Laplacian matrix, there is a change of coordinates $E(t) = \Phi[\nu_1(t), \nu_2(t)]^\top$ with Φ constructed with eigenvectors of A, such that the linearized deviation error can be written as:

$$\begin{array}{rcl} \dot{\nu}_1(t) & = & [DF(s(t)) + \lambda_1 \kappa C]\, \nu_1(t) \\ \dot{\nu}_2(t) & = & [DF(s(t)) + \lambda_2 \kappa C]\, \nu_2(t) \end{array} \tag{25}$$

with $\lambda_1 = 0$ and $\lambda_2 = -2$ the eigenvalues of A. Since λ_1 corresponds to the synchronized solution $x(t) = y(t)$ is sufficient to prove that $\dot{\nu}_2(t) = [DF(s(t)) + \lambda_2 \kappa C]\, \nu_2(t)$ is asymptotically stable. Which can be done using the Lyapunov function

$$V(\nu_2(t)) = \nu_2(t)^\top \Pi \nu_2(t) \tag{26}$$

with $\Pi = \Pi^\top > 0$ a positive definitive matrix of appropriate dimension. The derivative along the second equation of (25) is:

$$\dot{V}(\nu_2(t)) = \nu_2(t)^\top \left([DF(s(t)) + \lambda_2 \kappa C]^\top \Pi + \Pi\, [DF(s(t)) + \lambda_2 \kappa C] \right) \nu_2(t) \tag{27}$$

Its time derivative of the Lyapunov function is strictly negative if

$$[DF(s(t)) + \lambda_2 \kappa C]^\top \Pi + \Pi\, [DF(s(t)) + \lambda_2 \kappa C] \leq -\tau_2 I_3 \tag{28}$$

with $\tau_2 > 0$. Then, choosing κ such that (28) is satisfied, the coupled system (7)-(8) becomes synchronized.

4 Numerical Simulations

To illustrate the above results, first, we consider two identical dynamical systems with self-excited attractors:

4.1 Synchronization self-excited attractors in drive-response configuration

Consider a Rössler system as the drive with $x_2(t)$ as the output:

$$\begin{array}{rcl} \begin{bmatrix} \dot{x}_1(t) \\ \dot{x}_2(t) \\ \dot{x}_3(t) \end{bmatrix} & = & \begin{bmatrix} -x_2(t) - x_3(t) \\ x_1(t) + 0.2 x_2(t) \\ 0.2 + x_1(t) x_3(t) - 5.7 x_3(t) \end{bmatrix} \\ w(t) & = & x_2(t) \end{array} \tag{29}$$

and the response system coupled to the second variable:

$$\begin{array}{rcl} \begin{bmatrix} \dot{y}_1(t) \\ \dot{y}_2(t) \\ \dot{y}_3(t) \end{bmatrix} & = & \begin{bmatrix} -y_2(t) - y_3(t) \\ y_1(t) + 0.2 y_2(t) - \kappa_{22}(y_2(t) - x_2(t)) \\ 0.2 + y_1(t) y_3(t) - 5.7 y_3(t) \end{bmatrix} \\ z(t) & = & y_2(t) \end{array} \tag{30}$$

The resulting error dynamics are locally asymptotically stable with $\kappa_2 = [0, 0.5, 0]^\top$. For the numerical simulations in Figure 10, the coupling gain κ_{22} is changed from zero to 0.5 after 150 time units.

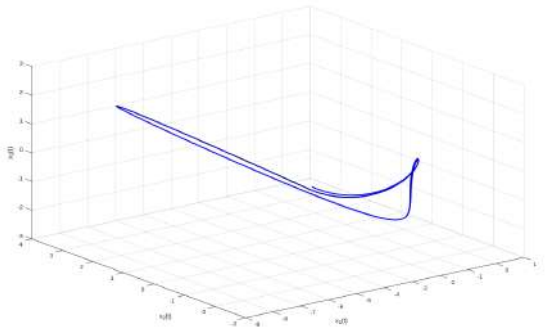

(a) Hidden attractor of system (33)

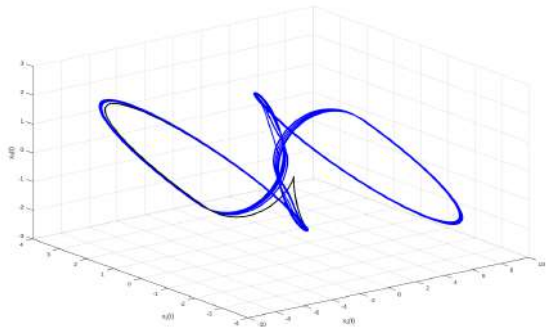

(b) Self-excited attractor of system (34)

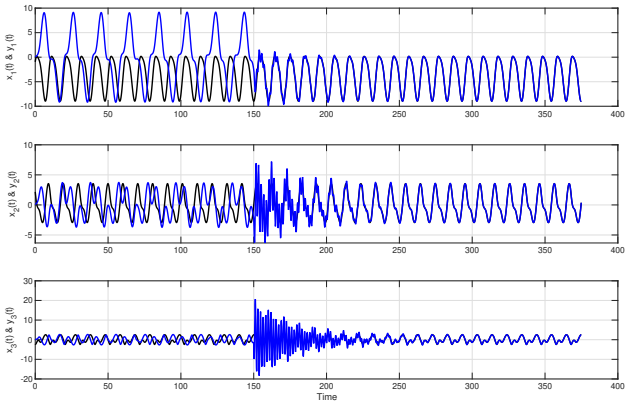

(c) State variables of the coexisting hidden and self-excited systems

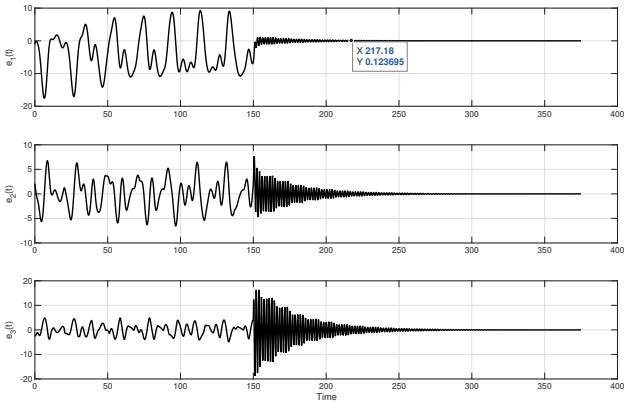

(d) Deviation error for the drive-response coupled systems with hidden and self-excited attractor

Figure 12: Synchronization of *drive-response* coupled hidden and self-excited systems for $\kappa_{22} = \kappa_{33} = 15$ for $t > 150$

4.2 Synchronization of self-excited attractors in bidirectional configuration

Consider two Lorenz systems coupled through their first coordinate:

$$\begin{bmatrix} \dot{x}_1(t) \\ \dot{x}_2(t) \\ \dot{x}_3(t) \\ w(t) \end{bmatrix} = \begin{bmatrix} 10(x_2(t) - x_1(t)) - \kappa_{11}(y_1(t) - x_1(t)) \\ 28x_1(t) - x_2(t) - x_1(t)x_3(t) \\ x_1(t)x_2(t) - \frac{8}{3}x_3(t) \\ x_1(t) \end{bmatrix} \tag{31}$$

And the response system coupled to the second variable:

$$\begin{bmatrix} \dot{y}_1(t) \\ \dot{y}_2(t) \\ \dot{y}_3(t) \\ z(t) \end{bmatrix} = \begin{bmatrix} 10(y_2(t) - y_1(t)) - \kappa_{11}(x_1(t) - y_1(t)) \\ 28y_1(t) - y_2(t) - y_1(t)y_3(t) \\ y_1(t)y_2(t) - \frac{8}{3}y_3(t) \\ y_1(t) \end{bmatrix} \tag{32}$$

The resulting deviation error dynamics are locally asymptotically stable with $\kappa = [50, 0, 0]^\top$. For the numerical simulations in Figure 11, the coupling gain κ_{11} is changed from zero to 50 after 150 time units.

As shown in Figure 10, for self-excited attractors synchronization between drive and response is achieved relatively fast once the coupling strength is set to $\kappa_2 = [0, 0.5, 0]^\top$. While for the bidirectionally coupled systems as shown in Figure 11, asymptotical synchronization is also achieved very fast on the synchronized solution once the coupling strength is set to $\kappa_1 = [50, 0, 0]^\top$. The previous simulation illustrates the solutions to the synchronization problem derived in the last Section. In the following subsections, we demonstrate how the presence of hidden attractors alters the expected synchronization outcomes in the case of coexisting attractors.

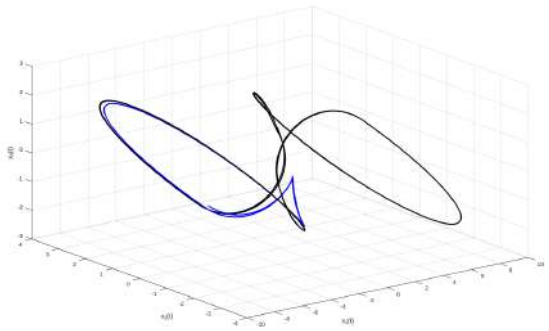

(a) Hidden attractor systems

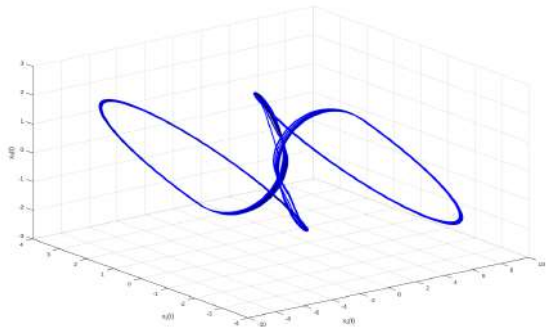

(b) Self-excited attractor

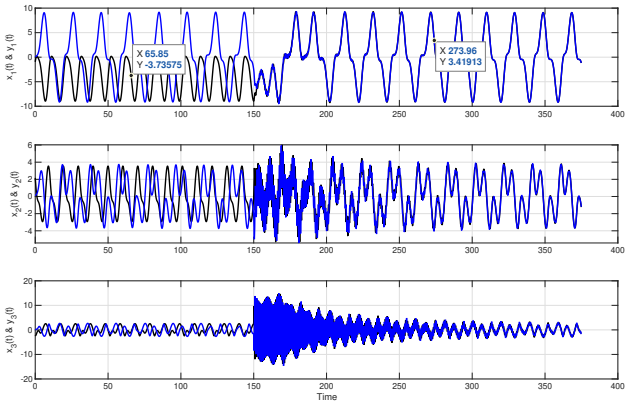

(c) State variables of the coexisting hidden and self-excited systems bidirectionally coupled

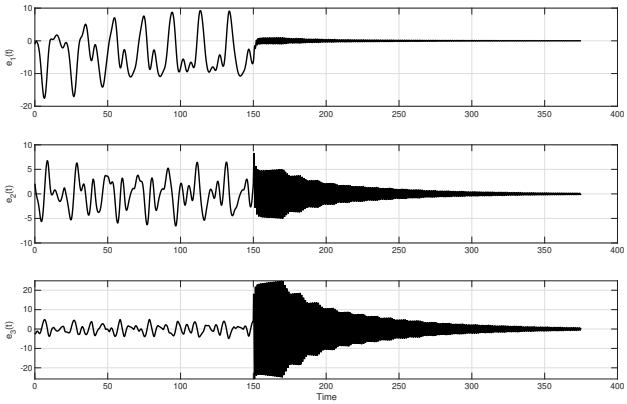

(d) Deviation error for the bidirectionally coupled systems with hidden and self-excited attractor

Figure 13: Synchronization of bidirectionally coupled hidden and self-excited systems for $\kappa_{22} = \kappa_{33} = 15$ for $t > 150$

4.3 Synchronization from hidden to self-excited attractor in drive-response configuration

In this case, we focus on systems that exhibit hidden and self-excited attractors. In particular, consider the case of PWL Jerk systems (6), where the hidden attractor is the drive and is coupled to the self-excited attractor with the second and third coordinates:

$$\begin{bmatrix} \dot{x}_1(t) \\ \dot{x}_2(t) \\ \dot{x}_3(t) \\ w(t) \end{bmatrix} = \begin{bmatrix} x_2(t) \\ x_3(t) \\ -0.7x_1(t) - 0.5x_2(t) - x_3(t) + F(x_1(t)) \\ x_2(t) + x_3(t) \end{bmatrix} \tag{33}$$

and bidirectionally coupled at their third variable:

$$\begin{bmatrix} \dot{y}_1(t) \\ \dot{y}_2(t) \\ \dot{y}_3(t) \\ z(t) \end{bmatrix} = \begin{bmatrix} y_2(t) \\ y_3(t) \\ -0.7y_1(t) - 0.5y_2(t) - y_3(t) + F(y_1(t)) - \kappa_{22}[x_2(t) - y_2(t)] - \kappa_{33}[x_3(t) - y_3(t)] \\ y_2(t) + y_3(t) \end{bmatrix} \tag{34}$$

In this case, the error dynamics are locally asymptotically stable for $\kappa = [0, 15, 15]^\top$, with the simulation results shown in Figure 12 where the coupling gains $\kappa_{22} = \kappa_{33}$ are changed from zero to 15 after 150 time units.

Notice that in Figure 12a, the hidden attractor is the drive system, and Figure 12b originally is on the self-excited attractor until the coupling gains are set to $\kappa = [0, 15, 15]^\top$, after that it moves to the hidden attractor and remains on it afterwards.

4.4 Synchronization from hidden to self-excited attractor in bidirectional configuration

Finally, we connect bidirectionally hidden and self-excited attractors in the PWL Jerk system of the form:

$$\begin{bmatrix} \dot{x}_1(t) \\ \dot{x}_2(t) \\ \dot{x}_3(t) \\ w(t) \end{bmatrix} = \begin{bmatrix} x_2(t) \\ x_3(t) \\ -0.7x_1(t) - 0.5x_2(t) - x_3(t) + F(x_1(t)) - \kappa_{22}[y_2(t) - x_2(t)] - \kappa_{33}[y_3(t) - x_3(t)] \\ x_2(t) + x_3(t) \end{bmatrix} \tag{35}$$

and bidirectionally coupled at their third variable:

$$\begin{bmatrix} \dot{y}_1(t) \\ \dot{y}_2(t) \\ \dot{y}_3(t) \\ z(t) \end{bmatrix} = \begin{bmatrix} y_2(t) \\ y_3(t) \\ -0.7y_1(t) - 0.5y_2(t) - y_3(t) + F(y_1(t)) - \kappa_{22}[x_2(t) - y_2(t)] - \kappa_{33}[x_3(t) - y_3(t)] \\ y_2(t) + y_3(t) \end{bmatrix} \tag{36}$$

The deviation error becomes locally asymptotically stable for $\kappa = [0, 15, 15]^\top$, with the simulation results shown in Figure 13 where the coupling gains $\kappa_{22} = \kappa_{33}$ is changed from zero to 15 after 150 time units.

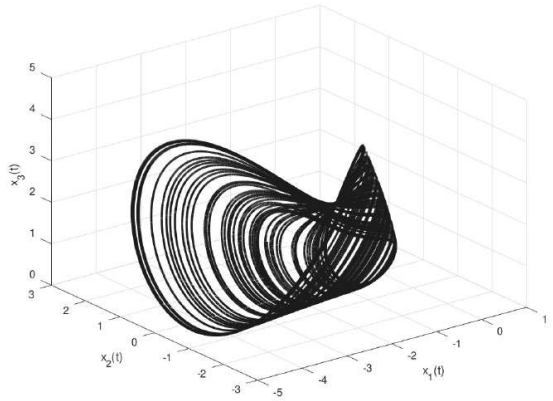

(a) Hidden attractor for system (37)

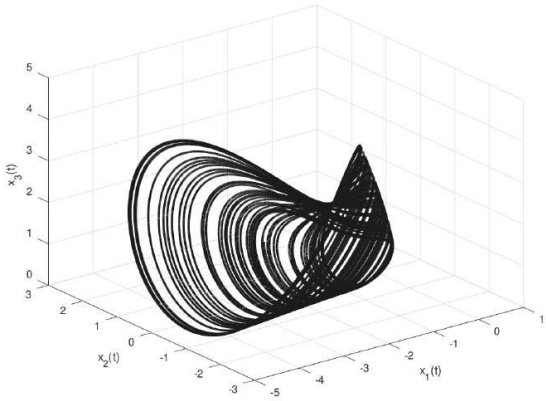

(b) Hidden attractor for system (38)

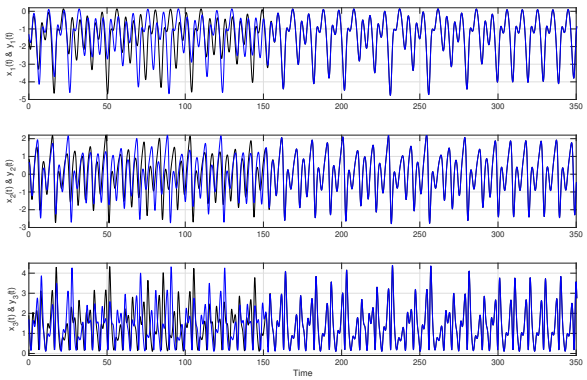

(c) State variables of the no equilibrium point system (1)

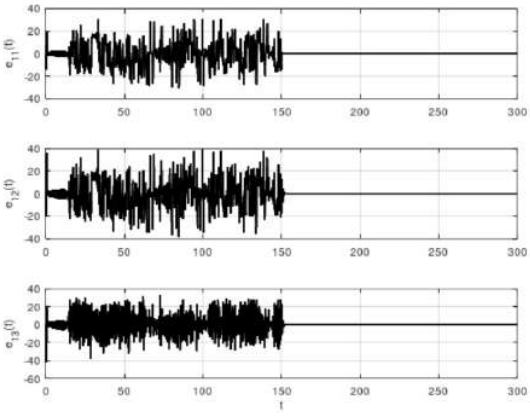

(d) Deviation error for the bidirectionally coupled no equilibrium systems

Figure 14: Synchronization error of bidirectionally coupled non-equilibrium point systems (1) for $\kappa_{33} = 5$ for $t > 150$

]

In the case of bidirectionally coupled systems with coexisting hidden and self-excited attractors. We start on the hidden attractor as shown in Figure 13a, while in Figure 13b begin as self-excited attractors, as the coupling strength change to $\kappa = [0, 15, 15]^\top$, the systems synchronize to the self-excited attractor since the effect of the connection moves the trajectories away from the hidden attractor an its basin of attraction and towards the self-excited. It is essential to note that the theoretical prediction that asymptotic synchronization due to the coupling remains valid,

but the solution where the synchronization emerges is the attractor with the basin of attraction that is visited in the transitory behavior of the coupled system.

4.5 Synchronization of hidden attractors in bidirectional configuration

Next, we consider two non-equilibrium point systems with hidden attractors (1), and output their second and third coordinates:

$$\begin{array}{rcl} \begin{bmatrix} \dot{x}_1(t) \\ \dot{x}_2(t) \\ \dot{x}_3(t) \end{bmatrix} & = & \begin{bmatrix} -x_2(t) \\ x_1(t) + x_3(t) \\ 2x_2(t)^2 + x_1(t)x_3(t) - 0.35 - \kappa_{22}[y_2(t) - x_2(t)] - \kappa_{33}[y_3(t) - x_3(t)] \end{bmatrix} \\ w(t) & = & x_2(t) + x_3(t) \end{array} \tag{37}$$

and bidirectionally coupled at their third variable:

$$\begin{array}{rcl} \begin{bmatrix} \dot{y}_1(t) \\ \dot{y}_2(t) \\ \dot{y}_3(t) \end{bmatrix} & = & \begin{bmatrix} -y_2(t) \\ y_1(t) + y_3(t) \\ 2y_2(t)^2 + y_1(t)y_3(t) - 0.35 - \kappa_{22}[x_2(t) - y_2(t)] - \kappa_{33}[x_3(t) - y_3(t)] \end{bmatrix} \\ z(t) & = & y_2(t) + y_3(t) \end{array} \tag{38}$$

In this case, the error dynamics are locally asymptotically stable for $\kappa = [0, 0, 5]^\top$, with the simulation results shown in Figure 14 where the coupling gains κ_{22}, κ_{33} are changed from zero to 5 after 150 time units.

In this case, the bidirectionally coupled systems have only hidden attractors. Therefore, even if the transitory behavior moves away from the hidden attractors initially, as the error approaches zero, there is only one basin of attraction, and both systems converge to the hidden attractor. Our results show that our theoretical predictions for the emergence of synchronization remain valid. Synchronization in bidirectionally coupled systems with hidden attractors is possible when there is no competition between basins of attraction.

5 Closing remarks

Based on Lyapunov stability analysis, we proposed solutions to the synchronization problem for two dynamical systems with hidden and self-excited attractors, in both drive-response and bidirectional coupling configurations. For systems with self-excited attractors, whether in drive-response or bidirectional coupling, asymptotic identical synchronization is achieved. However, in systems where hidden and self-excited attractors coexist, we observe that, in the drive-response configuration, it is possible to achieve synchronization by forcing the systems to synchronize on the hidden attractor. But in the bidirectional configuration, the synchronized behavior moves towards the self-excited attractor. Our numerical results suggest that hidden attractors have a small region of attraction that effectively reduces to the actual hidden attractor. Therefore, in the bidirectional configuration, the area of attraction of the hidden attractor merges with that of the self-excited attractor, making the synchronized behavior converge towards the self-excited attractor. In systems with only a hidden attractor, synchronization is achieved among hidden attractors because there is no such competition. In future investigations, we plan to address synchronization in networks of chaotic systems with coexisting hidden and self-excited attractors.

Conflicts of interest

Authors declare no conflicts of interest with respect to this article.

References

[1] S. H. Strogatz. *Nonlinear dynamics and chaos: with applications to physics, biology, chemistry, and engineering*. CRC press, 2018.

[2] G. A. Leonov and N. V. Kuznetsov. "From hidden oscillations in Hilbert-Kolmogorov, Aizerman, and Kalman problems to hidden chaotic attractors in Chua circuits". In: *International Journal of Bifurcations and Chaos* 23.1 (2013), pp. 1–69.

[3] N. V. Kuznetsov and G. A. Leonov. "Hidden attractors in dynamical systems: systems with no equilibria, multistability and coexisting attractors". In: *Proceedings of 19th World Congress IFAC*. Cape Town, South Africa, 2014, pp. 5445–5454.

[4] J. C. Sprott. "Some simple chaotic flows". In: *Physical Review E* 50.2 (1994), R647–R650.

[5] Z. Wei. "Dynamical behaviors of a chaotic system with no equilibria". In: *Physics Letters A* 376.2 (2011), pp. 102–108.

[6] X. Hu et al. "Multi-scroll hidden attractors in improved Sprott A system". In: *Nonlinear Dynamics* 86 (2016), pp. 1725–1734.

[7] S. Jafari and J. C. Sprott. "Simple chaotic flows with a line equilibrium". In: *Chaos, Solitons & Fractals* 57 (2013), pp. 79–84.

[8] M. A. Jafari et al. "Chameleon: the most hidden chaotic flow". In: *Nonlinear Dynamics* 88 (2017), pp. 2303–2317.

[9] X. Wang and G. Chen. "A chaotic system with only one stable equilibrium". In: *Communications in Nonlinear Science and Numerical Simulation* 17.3 (2012), pp. 1264–1272.

[10] Q. Yang and G. Chen. "A chaotic system with one saddle and two stable node-foci". In: *International Journal of Bifurcations and Chaos* 18.5 (2008), pp. 1393–1414.

[11] D. Dudkowski et al. "Hidden attractors in dynamical systems". In: *Physics Reports* 637 (2016), pp. 1–50.

[12] R. J. Escalante-González and E. Campos-Cantón. "Multistable systems with hidden and self-excited scroll attractors generated via piecewise linear systems". In: *Complexity* 2020.7832489 (2020), pp. 1–12.

[13] F. Delgado-Aranda et al. "Multistable systems with hidden and self-excited scroll attractors generated via piecewise linear systems". In: *Revista Mexicana de Física* 66.5 (2020), pp. 683–691.

[14] R. J. Escalante-González and E. Campos-Cantón. "Emergence of Hidden Attractors through the Rupture of Heteroclinic-Like Orbits of Switched Systems with Self-Excited Attractors". In: *Complexity* 2021.5559913 (2021), pp. 1–24.

[15] A. Pikovsky, M. Rosenblum, and J. Kurths. *Synchronization: A Universal Concept in Nonlinear Sciences*. Cambridge U. Press, 2001.

[16] S. Boccaletti et al. "The synchronization of chaotic systems". In: *Physics Reports* 366 (2002), pp. 1–101.

[17] L. M. Pecora and T. L. Carroll. "Synchronization in chaotic systems". In: *Physical Review Letters* 64.8 (1990), pp. 821–824.

[18] D. I. Rosas Almeida, Jq. Álvarez, and J. G. Barajas-Ramírez. "Robust synchronization of Sprott circuits using sliding mode control". In: *Chaos, Solitons & Fractals* 30.1 (2006), pp. 11–18.

[19] A. Roldán-Caballero et al. "Synchronization of a New Chaotic System Using Adaptive Control: Design and Experimental Implementation". In: *Complexity* 2023.1 (2023), p. 2881192.

[20] P. S. Skardal, D. Taylor, and J. Sun. "Optimal Synchronization of Complex Networks". In: *Physical Review Letters* 113.14 (2014), p. 144101.

[21] S. Boccaletti et al. "Complex networks: Structure and dynamics". In: *Physics Reports* 424 (2006), pp. 175–308.

[22] H. Su and X. Wang. *Pinning Control of Complex Networked Systems Synchronization, Consensus and Flocking of Networked Systems via Pinning*. Springer, 2013.

[23] U. Chaudhuri and A. Prasad. "Complicated basins and the phenomenon of amplitude death in coupled hidden attractors". In: *Physics Letters A* 378 (2014), pp. 713–718.

[24] V. T. Pham, C. Volos, and T. Kapitaniak. *Systems with hidden attractors: From theory to realization in circuits*. Springer, 2017.

[25] S. Zhang and Y. Zeng. "A simple Jerk-like system without equilibrium: Asymmetric coexisting hidden attractors, bursting oscillation, and double full Feigenbaum remerging trees". In: *Chaos, Solitons & Fractals* 120 (2019), pp. 25–40.